



THE UNIVERSITY *of* EDINBURGH

Edinburgh Research Explorer

Improving the Sampling Strategy for Point-to-Point Line-Of-Sight Modelling in Urban Environments

Citation for published version:

Bartie, P & Mackness, W 2016, 'Improving the Sampling Strategy for Point-to-Point Line-Of-Sight Modelling in Urban Environments' *International Journal of Geographical Information Systems*. DOI: 10.1080/13658816.2016.1243243

Digital Object Identifier (DOI):

[10.1080/13658816.2016.1243243](https://doi.org/10.1080/13658816.2016.1243243)

Link:

[Link to publication record in Edinburgh Research Explorer](#)

Document Version:

Peer reviewed version

Published In:

International Journal of Geographical Information Systems

General rights

Copyright for the publications made accessible via the Edinburgh Research Explorer is retained by the author(s) and / or other copyright owners and it is a condition of accessing these publications that users recognise and abide by the legal requirements associated with these rights.

Take down policy

The University of Edinburgh has made every reasonable effort to ensure that Edinburgh Research Explorer content complies with UK legislation. If you believe that the public display of this file breaches copyright please contact openaccess@ed.ac.uk providing details, and we will remove access to the work immediately and investigate your claim.



Improving the Sampling Strategy for Point-to-Point Line-Of-Sight Modelling in Urban Environments

Phil Bartie and William Mackaness
email: phil.bartie@stir.ac.uk

Abstract: Visibility modelling calculates what an observer could theoretically see in the surrounding region based on a digital model of the landscape. In some cases it is not necessary, nor desirable, to compute the visibility of an entire region (i.e. a viewshed), but instead it is sufficient and more efficient to calculate the visibility from point-to-point, or from a point to a small set of points, such as computing the intervisibility of predators and prey in an agent based simulation. This paper explores how different line-of-sight (LoS) sample ordering strategies increases the number of early target rejections, where the target is considered to be obscured from view, thereby improving the computational efficiency of the LoS algorithm. This is of particular importance in dynamic environments where the locations of the observers, targets and other surface objects are being frequently updated. Trials were conducted in three UK cities, demonstrating a robust five-fold increase in performance for two strategies (hop, divide and conquer). The paper concludes that sample ordering methods do impact overall efficiency, and that approaches which disperse samples along the LoS perform better in urban regions than incremental scan methods. The divide and conquer method minimises elevation interception queries, making it suitable when elevation models are held on disk rather than in memory, while the hopping strategy was equally fast, algorithmically simpler, with minimal overhead for visible target cases.

Keywords: *visibility analysis; LBS; urban modelling; line of sight; sample ordering*

1 Introduction

Visibility modelling is used to calculate what is theoretically visible from a specified location, with consideration given to the observer's height and surrounding topography. Increasingly surface objects (e.g. buildings, vegetation) are included in surface models

35 derived from Light Detection and Ranging (LiDAR) point clouds, expanding the range
36 of uses of visibility analysis in urban regions. Viewshed analysis calculates the regions
37 visible from a specific location, requiring every cell in a raster surface to be accessed
38 making it computationally expensive. However it is not always necessary to calculate
39 the visibility from an observer to a region, but instead the visibility between defined
40 point locations. For example computing the intervisibility between vehicles in an urban
41 transport simulation, or animals in a predator-prey agent based model (ABM), requires
42 visibility to be modelled from each observer's viewpoint. In such cases computing the
43 viewshed (i.e. region visible) for each observer would be very computationally
44 expensive and highly inefficient as much of the calculation time would be spent
45 computing the visibility of cells not relevant to the result. This is particularly relevant in
46 dynamic multi-observer simulations where the locations of agents (e.g. cars, people) are
47 frequently updated. In these instances point-to-point ray casting offers a more suitable
48 solution, by determining if an unbroken line-of-sight (LoS) exists between set members.

49 This research assesses the impact that the sample order has on performance in
50 point-to-point LoS calculations for urban regions, where only a Boolean target visibility
51 result is required (i.e. target is visible or not visible). The paper begins with a review of
52 visibility modelling, followed by a short introduction to the LoS model implementation,
53 before exploring a variety of LoS sampling strategies. The sample order strategies are
54 variations of the order in which points along the LoS are tested to determine if the target
55 is visible or not. An ideal sampling strategy would be one that consistently resulted in
56 early rejection of obscured targets (i.e. it avoids scanning all intermediate elevation
57 values between object and target). Five different sampling orders were assessed across
58 three UK cities, concluding that fivefold performance gains were possible where a
59 divide and conquer or hopping method were used. The hopping method included a
60 parameter for hop size, and trials showed that hop sizes of 20 to 30 metres were optimal
61 in urban regions. An explanation for this was sought by constructing synthetic city
62 elevation models of varying road width, revealing a strong positive correlation between

63 hop size and road width. The paper concludes with comments about how the LoS
64 performance improvement may be used, with suggestions for follow up research.

65

66 **2 Background**

67 Visibility modelling is included in the majority of Geographic Information Systems
68 (De Smith *et al.* 2007), and has become one of the most commonly used analysis tools
69 (Davidson *et al.* 1993). It is used for a range of research including landscape planning
70 (Fisher 1996), locating the most scenic or most hidden routes (Stucky 1998), siting
71 radio masts and wind turbines (De Floriani *et al.* 1994a), modelling spatial openness in
72 built environments (Fisher-Gewirtzman and Wagner 2003), and in military exercises as
73 a weapon surrogate (Baer *et al.* 2005).

74 Isovists (Tandy 1967, Benedikt 1979, Turner *et al.* 2001) have tended to be used in
75 modelling urban visibility where a map of building footprints is available but for which
76 there is no height information. In these cases the heights of the buildings are considered
77 to be infinite, and the limits of visibility are determined by a building's walls. A better
78 approximation of visibility is possible when a Digital Surface Model (DSM) is
79 available, typically collected using LiDAR, offering a 2.5D dataset that includes the
80 height of surface objects such as buildings and vegetation. In these cases a viewshed
81 (Tandy 1967, Lynch 1976) may be calculated which shows the regions visible from a
82 specified observation location.

83 The computational efficiency of isovist and viewshed models has received much
84 attention (De Floriani *et al.* 2000, Rana and Morley 2002, Rana 2003, Ying *et al.* 2006).
85 If every terrain cell in a line-of-sight path is considered between an observer and target
86 it is referred to as the 'golden case' (Rana and Morley 2002). This approach can be
87 computationally expensive; techniques have therefore been developed to reduce the
88 number of calculations by considering only visually important cells. For example a
89 Triangulated Irregular Network (TIN) (De Floriani and Magillo 1994) represents the

90 terrain as triangles and can be used to reduce surface noise by only depicting large
91 elevation changes. This and other terrain filtering techniques, can be used to reduce the
92 number of observer-target pairs considered in viewshed generation (Rana and Morley
93 2002) but are more suited to rural landscapes than the densely varied urban landscape.

94 The efficiency of viewshed algorithms may also be improved (Seixas *et al.* 1999),
95 including strategies such as sweeping LoSs to a set of perimeter cells a fixed distance
96 from the observer (Franklin and Ray 1994), replacing sightlines with reference planes
97 (Wang *et al.* 2000), and using voxels (Carver and Washtel 2012). There are also
98 benefits from maintaining partial blocking information using a balanced binary search
99 tree (Van Kreveld 1996), or lists (Andrade *et al.* 2011), to reduce duplication in the
100 computation of visibility for multiple LoSs passing over a cell.

101 Furthermore processing times may be reduced by parallelisation across multiple
102 cores (De Floriani *et al.* 1994b), across distributed systems (Mills *et al.* 1992), or on a
103 Graphics Processing Unit (GPU) (Xia *et al.* 2010, Gao *et al.* 2011). The reduction in
104 wall-clock time is not due to greater efficiency but from the computation being divided
105 into tasks that run concurrently on multiple processing cores.

106 Historically visibility modelling research has focussed on rural settings using digital
107 elevation models of the bare earth topography, but the situation has changed with the
108 availability of LiDAR datasets that also capture surface features (e.g. buildings). The
109 morphology of urban regions is quite different to rural regions, with more rapid
110 elevation changes between buildings and streets, forming more densely packed ridges
111 and valleys (Gal and Doytsher 2012). While the best views in rural areas are from the
112 higher elevations (hilltops), in urban space the observer is usually in the equivalent of a
113 ‘valley’, between the buildings, where dramatic changes in the visibility of features and
114 landmarks can fall in and out of view in a matter of a few strides. As a result there is a
115 need to revisit visibility modelling algorithms for a range of new uses in these
116 environments. Consider for example the requirement of a location based game running
117 on a smartphone, which can model user intervisibility. For such an application each user
118 would provide a location (point) and require a list of which users should be visible,

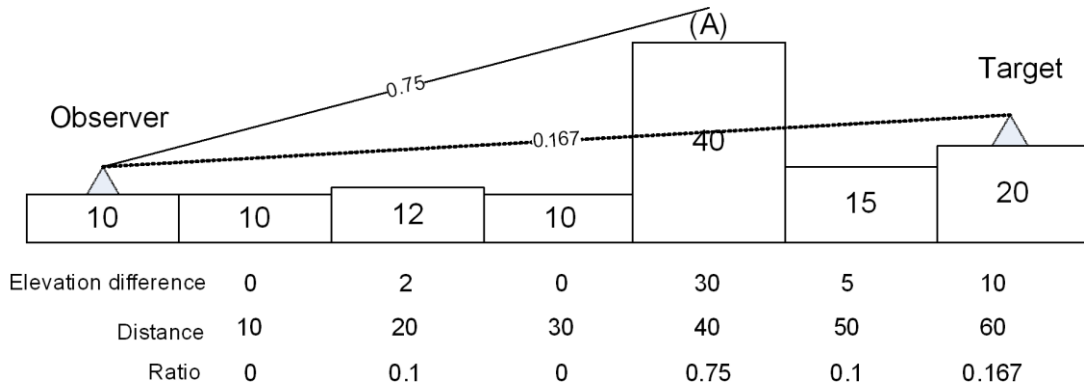
119 without the cost (limited CPU and battery life) of determining all surrounding visible
120 regions. Other applications of point-to-point visibility modelling include modelling the
121 view to junctions, traffic and signals, for vehicle navigation systems (Bartie and Kumler
122 2010, Tarel *et al.* 2012), GNSS shadow matching (Groves 2011), label removal for
123 obscured features in Augmented Reality applications (e.g. Nokia City Lens), and
124 simulations where more lifelike interactions are modelled by including visibility (e.g.
125 predator - prey ABM, transport simulations). In these cases each observer and target can
126 be adequately represented by a point location on the map surface, and visibility
127 calculated using a LoS between those locations. This paper focuses on that aspect of
128 visibility modelling, to improve the efficiency of point-to-point LoS modelling for
129 urban environments in anticipation of their growing use within highly dynamic
130 applications.

131 **3 Line of Sight Calculation**

132 LoS algorithms compare the vertical angle created from an observer to a specified target
133 at another location, against the vertical angles from the observer to all cells in between
134 (Fisher 1993). To reduce the computational cost, only the ratios need to be compared
135 rather than actual angles. If any intermediate cell creates a viewing ratio greater than
136 that of the observer to target ratio, then the target is considered to be obscured (Figure
137 1). The assumption is that the target is considered to be visible until proven otherwise,
138 and that the ratio from observer to target is the first calculation to which all other ratios
139 are compared. As soon as an intermediate viewing ratio is calculated above that of the
140 target, then the search may be aborted as the target has been shown to be obscured from
141 the observer (for example in Figure 1, $0.75 > 0.167$ indicating an obscured target).

142

143



144

145

146 *Figure 1: A line-of-sight approach calculating view ratios from observer to target.*
 147 *The ratio from observer to target is lower than to cell (A) therefore the target is*
 148 *obscured.*

148

149

150

151

152

153

154

155

156

157

158

If every terrain cell in a line-of-sight path is considered between an observer and target it is referred to as the ‘golden case’ (Rana and Morley 2002), but for a Boolean point-to-point visibility result these intermediate values are not required. A simple sampling strategy is to check the ratio for each cell incrementally from the observer to the target and determine if the target cell is obscured. If it is not blocked then the next intermediate cell is tested, until either all cells along the line-of-sight have been checked and the target is considered visible, or the target is calculated to be below the current view ratio and therefore obscured from view, resulting in early scan termination. This research seeks to find if the sample ordering strategy yields performance gains for point-to-point LoS calculations in urban environments.

159

160

161

162

163

164

165

166

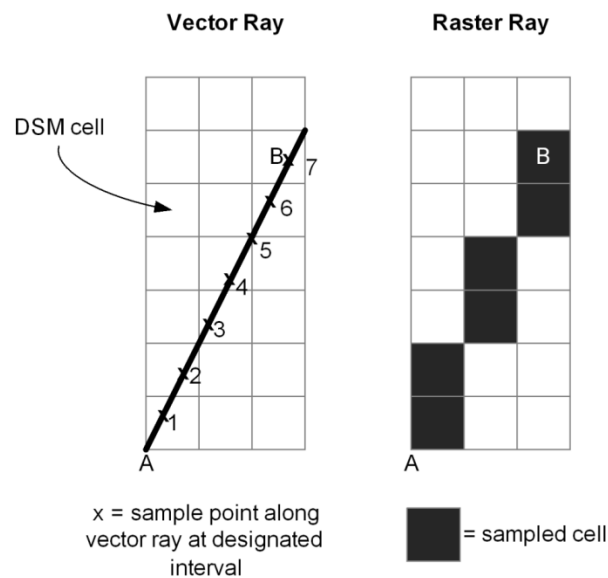
It is important to acknowledge the impact of data structure and type on the implementation. Elevation data may be stored as a Digital Elevation Model (DEM) or a Triangulated Irregular Network (TIN) (Lee 1991); each model has associated benefits and drawbacks (Kumler 1994). For this urban study a high resolution (1 metre) DSM, based on a LiDAR dataset, was found to be more suitable than using a TIN equivalent. To maintain the vertical resolution the TIN equivalent become extremely large, and despite using spatial indexes the ray-surface intercept performance was found to be significantly inferior. This was probably a result of the complexity of the urban

167 morphology which can be more easily represented in a cell based data format where
 168 indexes are implicit, and ray-surface intercepts may be retrieved more rapidly.

169 4 Line of Sight Sampling

170 There are a number of ways to sample the values from DSM cells between an observer
 171 and target. These include using a vector line which is sampled at given intervals along
 172 its length (Figure 2a – vector ray), and a raster approach such as the Bresenham's line
 173 algorithm, which uses integer addition to determine sample cells in order along a path
 174 from an observer to a designated target (Figure 2b – raster ray).

175



176

177

178 *Figure 2: Cell sampling approaches based on (a) vector and (b) raster lines*

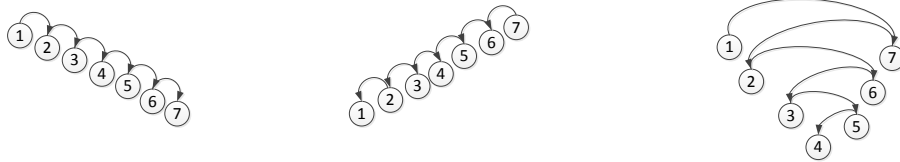
179

180 For this research the vector approach was adopted due to the ease with which sample
 181 locations can be re-ordered. Samples were located by projecting a point from the
 182 observer (Figure 2a - point A) a given distance, determined by the sample method used,
 183 at a specified angle towards the target (Figure 2a - point B). The sample ordering
 184 approaches used are illustrated in Figure 3. These were the normal forward incremental
 185 ordering (A) and reverse ordering (B), to test if obstructions near the observer or target

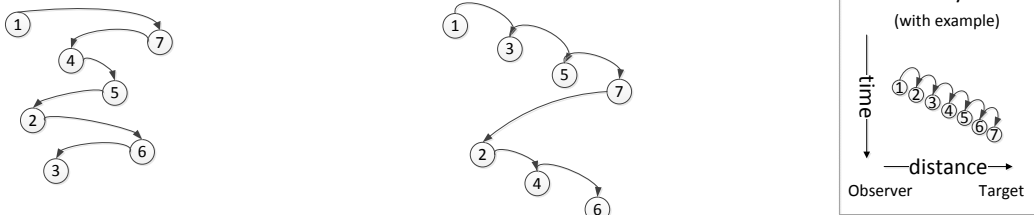
186 would result in early-target rejection. A first/last (C) sampling strategy was also
 187 included to give equal weighting to cells near the observer and cells near the target. For
 188 a more even priority across the length of the LoS a divide and conquer sample approach
 189 was used (D) which recursively divided the LoS by half, and a hopping strategy (E)
 190 whereby samples were taken at intervals (e.g. every 2m) along the LoS from the
 191 observer to the target. In cases where the target was visible each method would result in
 192 all intermediate sample locations being scanned.

193

A) Straight Ordering – e.g. 1234567 B) Reverse Ordering – e.g. 7654321 C) First, Last Ordering – e.g. 1726354



D) Divide and Conquer - e.g. 1745263 E) Hop of Length N – e.g. 1357246 (where N=2)



194

195 *Figure 3: Example outputs for each of the LoS sample orderings used*

196

197 The Python code to generate each sample order is shown below. The sample value is
 198 converted into a coordinate by projecting the value as a point along the LoS from the
 199 observer towards the target; a scaling factor may be introduced to accommodate
 200 different raster cell resolutions. The target's visibility is considered on each iteration
 201 until there are no more samples remaining (target visible), or the target is considered
 202 obscured (early rejection). The code for methods C and D are noticeably longer than the
 203 code required to implement the simpler incremental sampling strategies (A, B, E).

204

205

```
206 # [METHOD A] -- STRAIGHT ORDERING
207
208 tar_dist=distance(ObstoTar)
209
210 for s in range (1,tar_dist+1):
211     if (visibility(s)==False):
212         return False
213
214 return True
215
216 # [METHOD B] -- REVERSE ORDERING
217
218 tar_dist=distance(ObstoTar)
219
220 for s in range (tar_dist,0,-1):
221     if (visibility(s)==False):
222         return False
223
224 return True
225
226 # [METHOD C] -- FIRST, LAST ORDERING
227
228 tar_dist=distance(ObstoTar)
229
230 near_marker=0
231 far_marker=tar_dist+1
232
233 for d in range (1,tar_dist+1):
234     if (d%2!=0):
235         near_marker = near_marker+1
236         if (visibility(near_marker)==False):
237             return False
238
239     else:
240         far_marker = far_marker-1
241         if (visibility(far_marker)==False):
242             return False
243
244 return True
245
246 # [METHOD E] -- HOP ORDERING
247
248 tar_dist=distance(ObstoTar)
249 hop_n=2 #hop size in metres
250
251 for offset in range (1,hop_n+1):
252     for s in range (offset,tar_dist+1,hop_n):
253         if (visibility(s)==False):
254             return False
255
256 return True
```

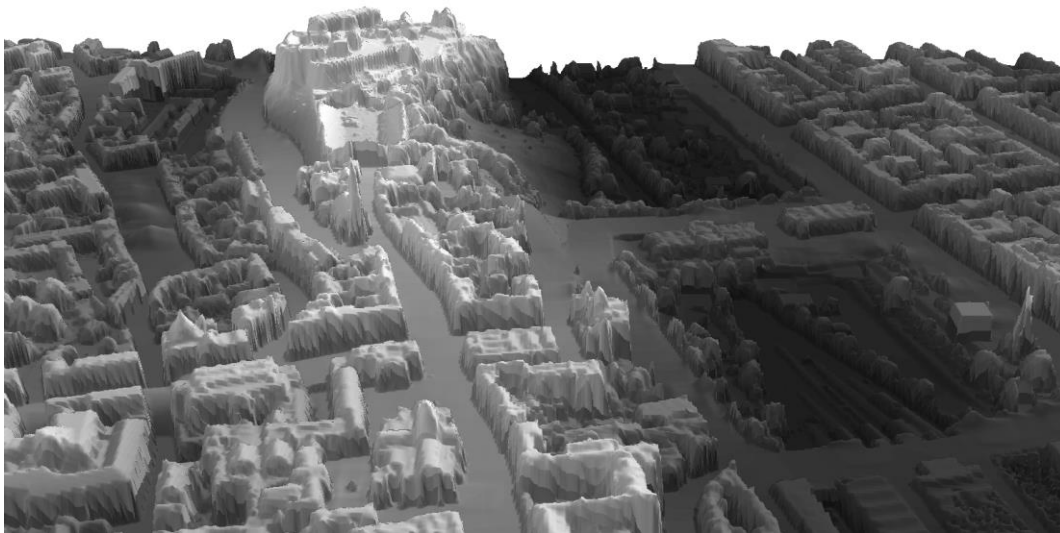
```

257
258 # [METHOD D] -- DIVIDE AND CONQUER ORDERING
259 class Node:
260     def __init__(self, l=None, r=None):
261         self.left=l
262         self.right=r
263
264     def midway(self):
265         return (self.right-self.left)/2 + self.left
266
267
268 class Queue (object):
269     def __init__(self, q=None):
270         if q is None:
271             self.q = []
272         else:
273             self.q = list(q)
274     def pop(self):
275         return self.q.pop(0)
276     def append(self, element):
277         self.q.append(element)
278     def length (self):
279         return len (self.q)
280
281 def div_conq (nodelist):
282     if (nodelist.length() >0):
283         current_node = nodelist.pop()
284         midway=current_node.midway()
285         if (visibility(midway)==False):
286             return False
287         if (midway < current_node.right-1):
288             n=Node(midway,current_node.right)
289             nodelist.append(n)
290         if (current_node.left < midway-1):
291             n=Node(current_node.left,midway)
292             nodelist.append(n)
293         return div_conq(nodelist)
294     else:
295         return True
296
297 # ----Main Routine----
298 tar_dist=distance(ObstoTar)
299 n=Node(1,tar_dist)
300 if (visibility(n.left)==False):
301     return False
302 if (visibility(n.right)==False):
303     return False
304
305 nodelist = Queue()
306 nodelist.append(n)
307 div_conq(nodelist)
308

```

309 For these trials the application ran on a single thread so that relative differences
310 in observed processing time were the result of changes to the sampling order, rather
311 than any parallelisation implementation. However, this is an embarrassingly parallel
312 case as observer-to-target LoS calculations could be run simultaneously across all
313 available CPU cores, for example sets of agents in an ABM could model visibility to
314 other agents in parallel limited only by the number of processing cores available.
315 Furthermore parallelisation may be included within each LoS so that sets of surface
316 intercept calculations are computed simultaneously; this would incur a minor
317 computational overhead when a thread had determined the target to be obscured making
318 other active threads redundant. However, these parallelisation solutions do not address
319 the issue central to this research – namely performance improvements from different
320 sampling order strategies and the reduction of processing overhead (e.g. to minimise
321 battery usage).

322 Trials were conducted using a PC with 3GB RAM and a 2.4GHz Intel Duo CPU
323 with power management set to high performance mode, recording the processor
324 execution time to avoid timing variations resulting from other OS background
325 processes. The software was written in C# .NET 4.5.1 using Visual Studio 2013 with
326 code optimisation enabled. The DSM was loaded into memory at the start of the
327 experiment to remove variations from disk activity. These initial trials were conducted
328 using a 6.7km by 4.3km DSM at 1m resolution for the city of Edinburgh, Scotland
329 (Figure 4).



330

331 *Figure 4: Perspective view of a section of Digital Surface Model used for trials in*
332 *Edinburgh (Scotland), looking towards Edinburgh Castle with Old Town on the left,*
333 *and New Town on the right*

334 **4.1 Trial 1 – Single Point to Point**

335 Random pairs of observer-target locations were selected within the study region
336 (Edinburgh) until a pair were found where the target was calculated to be visible using
337 the golden case (i.e. scanning all points along the LoS) and the observer was located in
338 a pedestrian accessible space (i.e. road, open space), to simulate observers at ground
339 level and avoid calculations from roof tops. The selected observer-target pair was a
340 distance of 1.2km apart, but to increase the workload for timing purposes the visibility
341 calculation was carried out 5000 times in succession without caching.

342 The results indicated no performance benefit among the approaches A,B,C and
343 E, as all intermediate cells are sampled between the observer and target (Table 1 –
344 Visible case). Minor performance differences are due to overheads in the ordering
345 algorithm implementations. Method D showed an increased calculation time (121%)
346 due to the more complex queueing and dequeuing methods required to generate the
347 sample order, as seen in the code outlined previously.

348 A second observer-target pair was then randomly chosen with the conditions of
 349 also being 1.2km apart and pedestrian accessible, but where the target was not visible.
 350 The CPU times for those calculations are shown in Table 1 (Not Visible case), and
 351 reveal significantly shorter calculation times than the visible case. These faster times
 352 result from early rejections made possible when a target is calculated to be obscured,
 353 and allowing the LoS to terminate before scanning all intermediate cells. The quicker
 354 execution times are evident for all methods, but the most significant performance gains
 355 arise from the methods that distribute the sampling locations along the ray length rather
 356 than scan incrementally (i.e. methods A,B,C). Notably Method D (divide and conquer)
 357 returned 'target obscured' in 13.2% of the time taken by Method A (straight ordering),
 358 while Method E (hop) completed the task in 27.2% of the time of Method A.

359 The performance benefits from the not visible case will be influenced by the
 360 specific topography and observer-target locations used in the trial but this initial trial
 361 does reveal differences in the overheads for visible cases, and that sample ordering does
 362 impact overall LoS efficiency. Further trials were undertaken with a random mix of
 363 visible and non-visible targets to establish the typical benefits from LoS sample
 364 reordering in urban landscapes.

365
 366
 367
 368
 369

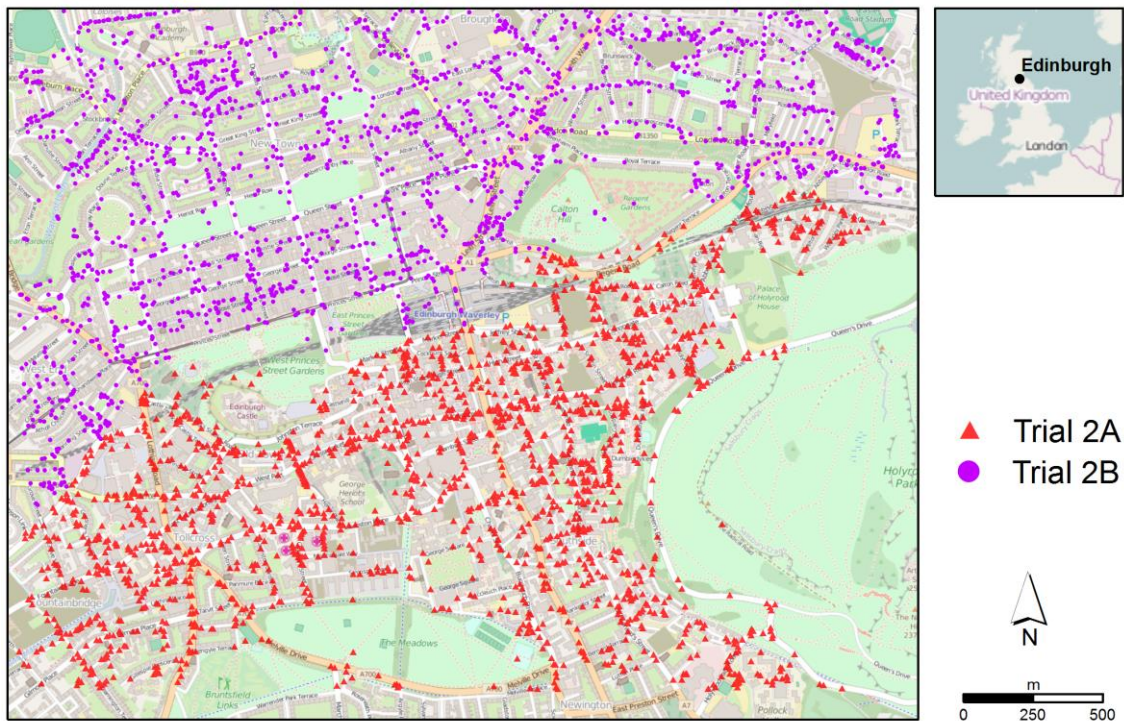
Table 1: Visibility trials using different sampling orders for a visible and non-visible observer-target pairs 1.2km apart. CPU times are given in seconds for 5000 trials, the hop distance (Method E) was 5m.

Case	Order	A	B	C	D	E (N=5m)
Visible	Time (sec)	3.837	3.900	3.884	4.648	3.900
	% of A	100.0	101.5	101.0	121.1	101.5
Not Visible	Time (sec)	0.114	0.202	0.233	0.015	0.031
	% of A	100.0	177.2	204.4	13.2	27.2

370 **4.2 Trial 2 – Multiple Observer-Target Pairs**

371 For the second set of trials, locations were selected randomly around Edinburgh city
 372 with a restriction that they must be in pedestrian accessible locations, as shown in
 373 Figure 5. Edinburgh is a hilly city, and consists of an Old Town with narrow winding
 374 streets (to the south), and a New Town (to the north) which has wider roads and a more
 375 grid like street pattern. Trial 2A was conducted using 2000 locations within the Old
 376 Town, while Trial 2B used 2000 locations within the New Town. The trials involved
 377 casting a LoS from each sample location to all others in that trial set, resulting in 4
 378 million ray casts per trial. An additional Trial 2C was conducted using the combined
 379 4000 locations to include views between Old and New Towns, resulting in 16 million
 380 rays cast.

381



382

383

384

385

*Figure 5: Randomly selected locations in Edinburgh (Scotland) for Trial 2
 (Background map: © OpenStreetMap contributors)*

386 A check was carried out after each trial to ensure the results matched the golden case
 387 (Method A). The calculations were not reflexive as an elevation offset of 1.8 metres was
 388 applied to the observer, to model the user’s eye-height, and an elevation offset of 0.5
 389 metres was applied to the target to reduce impact of minor data noise in the surface
 390 model. The results from these trials are shown in Table 2, with times given in seconds,
 391 and where the hop size for Method E was set to 5 metres.

392

393 *Table 2: Comparing the performance differences in sample order strategies for*
 394 *computing the visibility from locations around Edinburgh’s Old town (2A) and New*
 395 *town (2B) and the combined samples from both regions (2C). CPU times are given in*
 396 *seconds, and the hop distance for E was 5m.*

397

398

Trial	Sample Order	A	B	C	D	E (N=5m)
2A	Time (sec)	89.653	89.295	74.880	17.893	28.048
	% of A	100.0	99.6	83.5	19.9	31.3
2B	Time (sec)	86.892	99.232	80.683	16.348	30.076
	% of A	100.0	114.2	92.8	18.8	34.6
2C	Time (sec)	339.212	334.426	293.668	62.731	103.907
	% of A	100.0	98.6	86.6	18.5	30.6

399

400 As a percentage the calculation times are fairly consistent across the different trials,
 401 despite different street patterns and topography, ranking D, E, C, A/B in order of
 402 performance from most to least efficient.

403 This more comprehensive trial showed the additional computational overhead
 404 from sample reordering was outweighed in the majority of cases (i.e. all cases apart
 405 from 2B-B), and confirmed that the most impressive reductions resulted from strategies
 406 that spread the sample locations along the LoS – the divide and conquer approach (D),
 407 and the hop method (E).

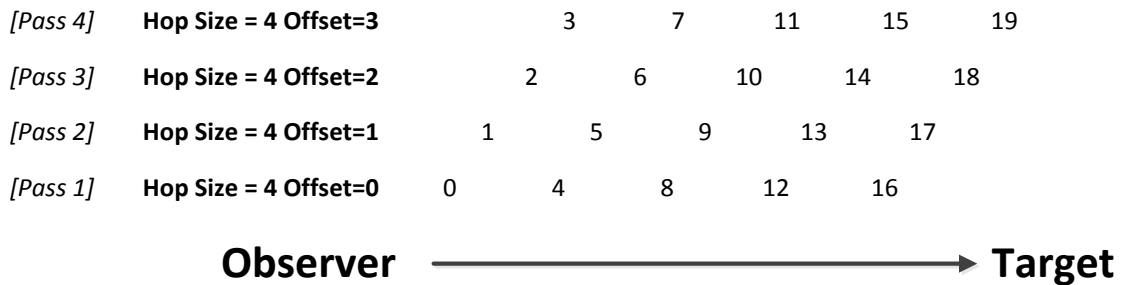
408 4.3 Trial 3 – Varying the hop size

409 In the previous example the hop size was set to 5 metres, however to determine if a
 410 more appropriate value could be used, two further trials were conducted using the same

411 random locations from Trials 2A and 2B but adjusting the hop size value on each run.
 412 As before each trial resulted in 4 million LoS to calculate the intervisibility between the
 413 2000 sample locations. The locations for these trials were centred on different parts of
 414 the city in order to assess the sensitivity of the hop value to urban morphology.

415 For larger hop sizes fewer samples are required on each pass but there is an
 416 increase in the number of subsequent ‘in filling’ passes to ensure that all the sample
 417 locations are sampled (Figure 6). This is necessary so that all cells are sampled along
 418 the LoS from observer to target in visible cases. The optimum hop size occurs when
 419 there is the highest chance of an early rejection of the target's visibility, when the tested
 420 viewing angle is greater than that of the target.

421



422

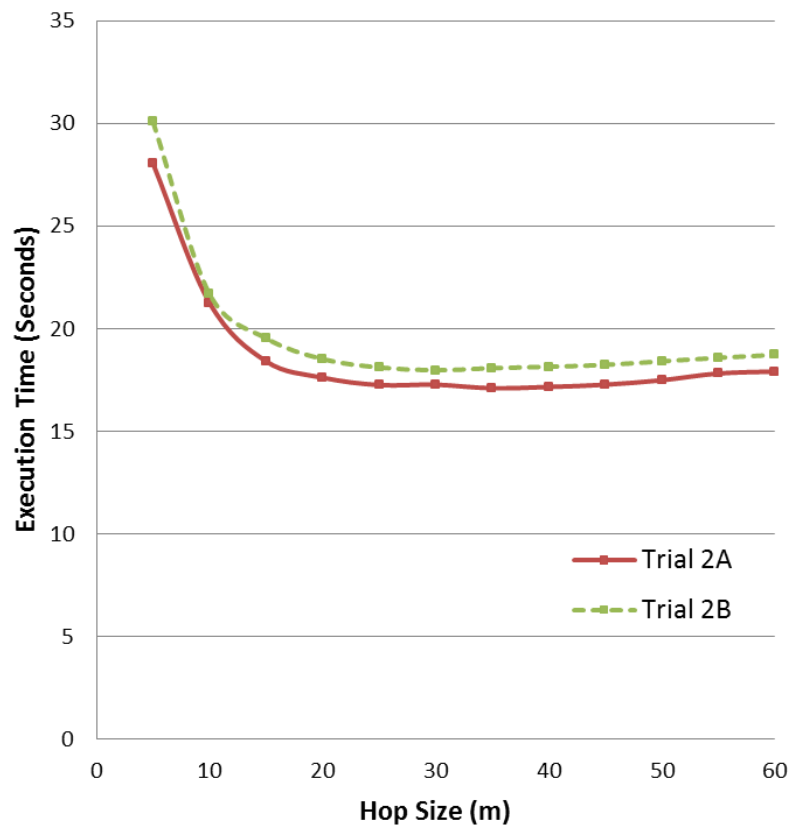
423 *Figure 6: Example of the hop sample ordering where hop size is 4 and the offset is*
 424 *incremented by 1*

425

426

427 The results from these two trials are shown in Figure 7, and exhibit very similar
 428 patterns, whereby the optimum hop size is between 25-35 metres. The optimal hop size
 429 for Trial 2A was 25m, while hops of 30m yielded marginally faster times in Trial 2B.
 430 The greatest performance gains are made until the hop size reaches 15m, after which
 431 there is a plateau until around 40 metres. Beyond 40m there is a marginal increase in
 432 execution time, as more infilling sample locations are required. In cases where the hop
 433 size is greater than the distance from observer-target then only the offset parameter
 434 plays a part, and effectively the sampling strategy mimics Method A (straight ordering).

435



436

437 *Figure 7: Execution times with varying hop sizes for two trials in different parts of*
 438 *Edinburgh City (Trial 2A - Old Town and Trial 2B - New Town)*

439

440

441 Table 3 summarises the findings for the improved sampling strategies D and E,
 442 compared to the incremental forward scan (A). After adjusting the hop sized this offered
 443 comparable speed improvements to the Divide and Conquer method, yet without any
 444 overheads in visible cases (as per Table 1).

445

446

447

448

449

450

451 *Table 3: Result Comparison Summary – Edinburgh trials*

452

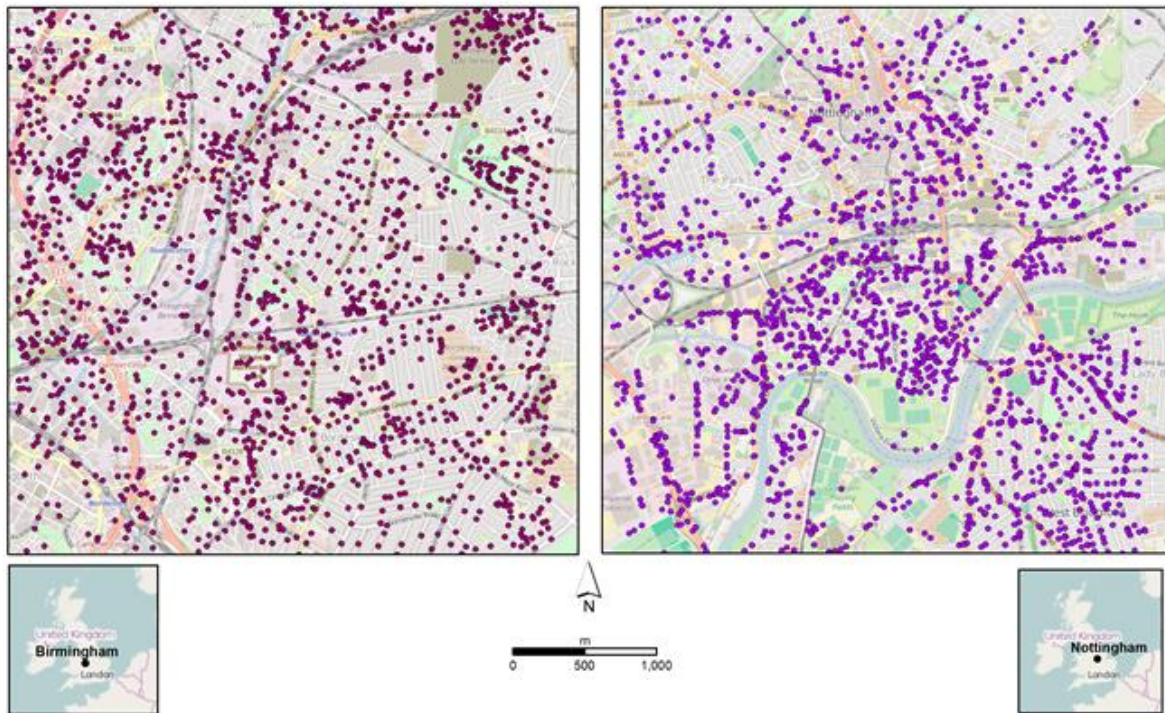
	Order	A	D	E	E
	Trial				
2A	Time	89.653	17.893	28.048	17.253
	(seconds)			(N=5m)	(N=25m)
	% of A	100	19.9	31.3	19.2
2B	Time	86.892	16.348	30.076	17.971
	(seconds)			(N=5m)	(N=30m)
	% of A	100	18.8	34.6	20.7

453

454

455 **4.4 Trials for Other Cities**

456 Further trials were undertaken in two other UK cities (Birmingham and Nottingham) to
457 determine if methods D and E exhibited similar performance benefits in different urban
458 morphologies. These cities were chosen due to their different street patterns,
459 topography, and the availability of LiDAR datasets from which 1 metre resolution
460 DSMs could be generated. The trials were conducted using a 4km by 4km region
461 around the city centre, and as before 2000 random pedestrian accessible locations were
462 selected around the city (Figure 8). As with the Edinburgh trials particular attention was
463 taken to ensure that sample locations did not fall on building or tree top locations. This
464 was done by rejecting randomly selected sample locations where focal statistics
465 indicated nearby road elevation values were more than 1m lower than the selected cell
466 (i.e. current road cell is 1 metre or more above the surrounding road level).



467

468 *Figure 8: Sample locations for Birmingham and Nottingham city trials*

469 (Background map: © OpenStreetMap contributors)

470

471 The intervisibility from each sample to all others within each city was calculated using
 472 Methods A-E (Table 4). The results exhibit a very similar pattern to that noted for the
 473 Edinburgh trials (Table 2).

474

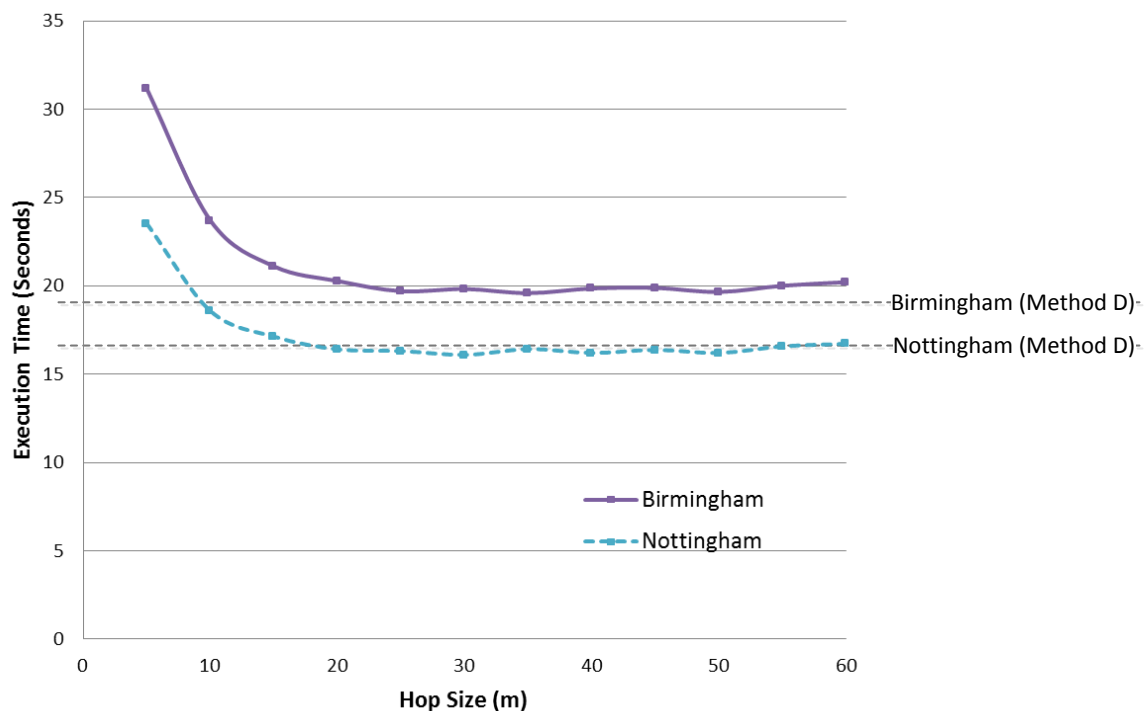
475 *Table 4: Visibility calculations times for each sampling methods in Nottingham and*
 476 *Birmingham cities*

Trial	Sample Order	A	B	C	D	E (N=5m)
Birmingham	Time (sec)	98.655	122.257	80.808	18.142	31.153
	% of A	100.0	123.9	81.9	18.4	31.6
Nottingham	Time (sec)	61.916	75.925	49.951	16.536	23.524
	% of A	100.0	122.6	80.7	26.7	37.9

477

478

479 As before method D shows the biggest performance improvement completing the
 480 calculations in 18.4% (Birmingham) and 26.7% (Nottingham) of method A. The
 481 optimum hop size was 30 metres for Nottingham, and 25 metres for Birmingham
 482 (Figure 9), though it should be noted that beyond 20m the impact on execution time is
 483 minimal and for this range of urban morphologies individualised hop sizes are not
 484 necessary.
 485



486
 487

488 *Figure 9: Trials to determine optimum hop size for Birmingham and Nottingham*
 489 *cities, showing Divide and Conquer times (Method D) for each city as a comparison*

490 These results for Birmingham and Nottingham show a similar trend to that noted in the
 491 Edinburgh trials, with processing times reducing significantly until the hop size reaches
 492 15 metres. From 20 metres upwards the performance benefits are fairly consistent, with
 493 a minor decrease in performance as the hop size increases above 50 metres.
 494

495

496 Based on the trials across three UK cities, of varying urban morphology, the results
 497 demonstrate a consistent performance improvement in using a Divide and Conquer
 498 approach, or a hopping strategy with a hop size of between 25 metres and 30 metres.

499

500

501

502 The DSM query rate can be calculated for each method as a ratio of the number of DSM
 503 queries required when casting a ray from observer to target divided by the processing
 504 time. Table 5 shows the average number of samples per millisecond achieved by each
 505 method, across all of the city trials. It reveals that despite the shorter processing times of
 506 the Divide and Conquer approach (D) it has the slowest sampling rate, due to the added
 507 complexity of the algorithm, meaning each iteration took longer. However as the
 508 number of iterations required was lower than other approaches this method would be
 509 the most suitable where DSM access had a high cost, such as for very large terrains
 510 stored on disk rather than in memory.

511

512 *Table 5: Efficiency of method based on DSM query rate*

Method	A	B	C	D	E
Average Samples per Millisecond	1398.4	1092.4	1344.7	689.6	1186.1

513

514 Based on the sample rates achieved it is possible to illustrate the benefit of using a
 515 point-to-point sampling strategy rather than generating a viewshed for each observer in
 516 multiple-observer scenarios where Boolean target visibility results are sufficient. At a
 517 rate of 1398 samples per millisecond (Method A) it would take at least 11 seconds to
 518 compute a viewshed for the 4km by 4km DSM at 1m resolution. As a comparison the
 519 same PC takes around 23 seconds to compute a viewshed using ESRI ArcGIS 10.2 for a
 520 single observer on the Birmingham DSM. Therefore to calculate a viewshed for each of
 521 the 2000 observers, to establish which targets are visible, would take in excess of 6

522 hours. In comparison the Boolean visibility of observer-target pairs using Ordering
523 Methods D or E is around 30 seconds or better (see Table 3 and Table 4). This illustrates
524 that despite possible repetitions of calculations for intermediate DSM cells there is still
525 a big advantage in using LoS rather than viewsheds in such applications.

526

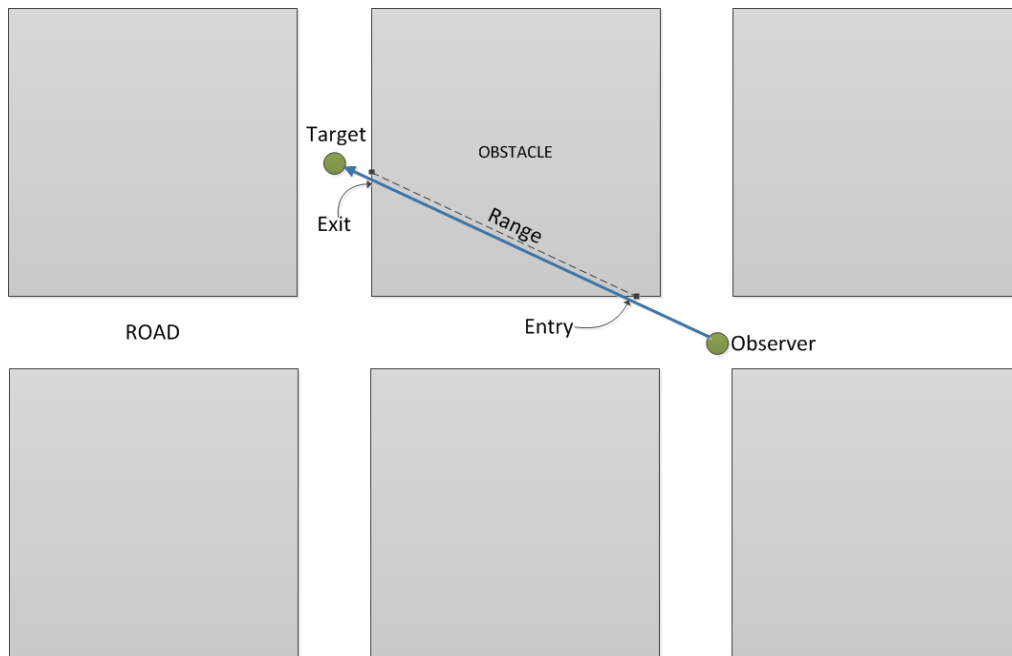
527 To gain a better understanding of the relationship between urban morphology and hop
528 size a further trial was undertaken using a synthetic city design, as explained in the next
529 section.

530

531 **4.5 Analysis of Results and Synthetic City Trials for the Hop Method (E)**

532 It is likely that the geographical scale of urban space has an impact on the hop size, as
533 despite differences in the average building sizes in the three cities (Birmingham 95.1 sq
534 m; Nottingham 95.7 sq.m; Edinburgh 143.0 sq.m) the road widths are similar at
535 between 15 metres and 30 metres wide. When you consider that the observer locations
536 are most probably near a road, it is likely that a sample will soon encounter a building
537 resulting in an early termination of the LoS. To gain a better understanding of the
538 relationship between hop length and road width, six synthetic cities were constructed.
539 These had a uniform grid structure with buildings of 80 metres by 80 metres. One
540 thousand pedestrian accessible points were chosen randomly, and the LoS from each to
541 all other locations were calculated (1 million LoS calculations per synthetic city). The
542 distance to the first interception with a blocking object (i.e. building) was recorded
543 along with the last interception with that object (Figure 10), giving a range of distances
544 for which a hop length would result in an early termination of the LoS. For example a
545 hop length of between 17m and 75m would result in an early LoS termination in the
546 synthetic city dataset with road widths of 10m (from Table 6).

547



548

549 *Figure 10: Illustration of the Entry and Exit Obstacle Distances for LoS in Synthetic*
 550 *City*

551

552

553 *Table 6: Relationship between Road Width and LoS Obstacle Distance for Synthetic*
 554 *Cities for 1 Million LoS calculations (see Figure 11).*

555

Road Width (m)	Observer to Obstacle Entry (m)	Observer to Obstacle Exit (m)	Range (m)
10	17	75	58
15	23	83	60
20	32	92	60
25	40	100	60
30	48	109	61
35	56	117	61

556

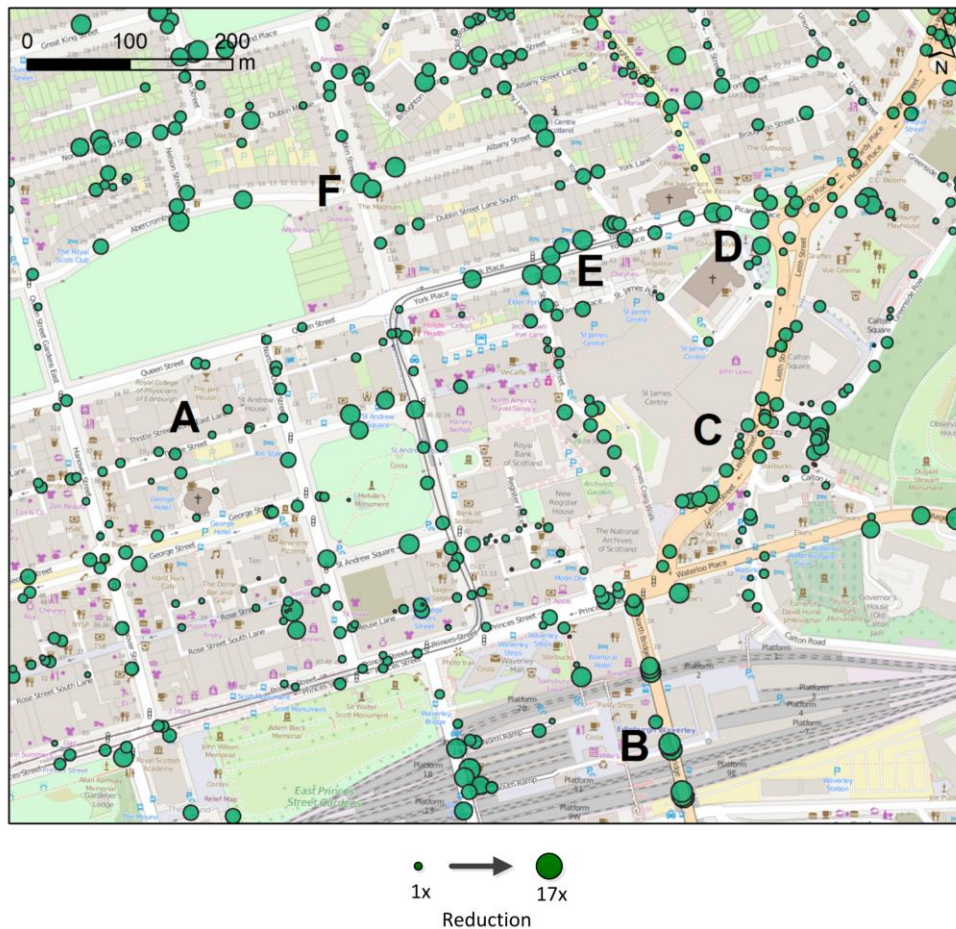
557 The Pearson product moment correlation between road width and the first obstacle
 558 distance is 0.999 (3dps), showing a very strong positive relationship that effective hop

559 size increases with wider roads. In these trials on synthetic cities the building size was
560 fixed at 80 metres by 80 metres in all cases, and it is interesting to note that the first
561 intersection was consistently around 1.6 times the road width, and the range was a fairly
562 consistent 60 metres in these cases with the 80 metre square buildings.

563 Analysis of the trial data exhibits similar patterns but with the added
564 complexities of a more diverse urban fabric and topography. Figure 11 shows the
565 geographical pattern of performance gains that can be made using a dispersed sample
566 strategy (here a comparison is made to Method E but the results are very similar for
567 Method D) as a result of the urban morphology when calculating the visibility to the
568 2000 target locations in Trial 2B. This section of New Town in Edinburgh was selected
569 as it demonstrated a range of interesting results within a small geographic region.

570 Narrow streets (e.g. Figure 11, A) have restricted views and require few samples
571 to determine target visibility, thereby limiting the efficiency gains possible. Similarly
572 when the observer is surrounded by tall buildings particular on curved roads (Figure 11,
573 C) the opportunity for sample reduction is minimal. The largest efficiency gains are
574 made in the more open expanses such as North Bridge (Figure 11, B), and where wide
575 entry and exit roads meet at a roundabout (Figure 11, D), on the longer wider straight
576 roads (Figure 11, E) and at junctions (Figure 11, F) where the space is more open giving
577 way to longer views. In these places the dispersed sampling strategies reduce the total
578 number of samples required dramatically (Method E up to 17 times reduction, while
579 Method D up to 47 times reduction for Trial 2B). The correlation in efficiency gains
580 between Method D and Method E (hop = 30m) when compared to Method A was 0.872
581 (3dps), indicating that both methods benefit similarly from the surrounding geography.

582 The overall performance of the various algorithms is a result of the reduction in
583 the number of samples required based on the geographic surroundings, and also the time
584 taken per sample based on the ordering efficiency. In narrow corridors the room for
585 performance improvement is minimal, while greater efficiencies can be made in the
586 more open spaces, along wider streets, and near junctions.



587

588 *Figure 11: An excerpt from the map of New Town, Edinburgh, showing the reduction*
 589 *for Trial 2B in total samples used by Method E ($N=30m$) compared to Method A*
 590 *(Background Map : © OpenStreetMap contributors)*

591

592

593 **5 Conclusion**

594 This research has shown that sampling order has a significant impact on the calculation
 595 times for computing Boolean visibility for observer-target pairs. The two most
 596 impressive performance improvements resulted from methods which distribute the
 597 samples from observer to target, rather than scan incrementally. A Divide and Conquer
 598 approach, which recursively subdivided the space, offered a robust fivefold increase in

599 execution performance, however the more complex algorithm overheads led to an
600 increase in processing times for visible cases. A hopping strategy also showed a fivefold
601 performance increase when using a sampling hop of around 30 metres, with minimal
602 processing overhead for visible cases. Trials in three UK cities revealed that the
603 improvement was robust for hop lengths in the range 20-40 metres. Future work could
604 compare the results across a wider range of cities in different parts of the world, and
605 also in more rural areas to determine the range of hop sizes suited to different
606 topographies. Trials on synthetic datasets indicate the hop length and road width are
607 strongly related. This fact considerably simplifies the tuning of the hop algorithm.

608 This work is not beneficial for searching for site locations where all cells in a
609 study region need to be calculated to determine suitable candidates. In these cases a
610 sweep algorithm would be more suitable (Franklin and Ray 1994, Andrade *et al.* 2011).
611 However the optimisation presented in this paper is suitable where a Boolean visibility
612 result is required in point-to-point scenarios, particularly in multi-observer dynamic
613 situations. This algorithm has been used successfully implemented in a client-server
614 setup to support natural language generation of wayfinding instructions for LBS clients,
615 and is soon to be included in an urban simulation package. Other examples of where it
616 could be used include person-to-person evasion (e.g. military applications), geosensor
617 networks (e.g. determining if other sensors are in direct line of sight), event triggering
618 (e.g. building entrance or junction visibility in LBS applications), location based
619 gaming, and simulations (e.g. crowd modelling, predator-prey agent based models).
620 Salomon *et al* (2004) suggested that up to 40% of processing time can be attributed to
621 LoS queries in simulations, and there is an increasing need to optimise as advances in
622 acquisition and storage technologies have enabled ever greater precision in reality
623 modelling with a commensurate increase in the number of obstacles against which LoS
624 queries must be tested.

625 There are also benefits for client-server setups where a server may be supporting
626 many concurrent users (e.g. friends in view on a location based service), or where
627 calculations are carried out on mobile devices with more limited processing and power

628 resources (e.g. smartphone clients). In these cases reducing the actual computation
629 (rather than increasing available processing power through parallelisation) significantly
630 reduces power consumption.

631 This work has assessed the relative efficiency of LoS algorithms for ‘visible /
632 not visible’ cases in the context of urban environments. The work has wide ranging
633 importance particularly in the context of highly dynamic urban environments where
634 mobile devices are required to process very large volumes of data, and agent based
635 modelling. It is also relevant to applications that span gaming (in real and synthetic
636 worlds), location based services, and augmented reality more generally. Future work
637 will look at its suitability in rural areas, where the topography is less angular and more
638 softly undulating.

639 **6 Acknowledgements**

640 The research leading to these results has received funding from the EC’s 7th
641 Framework Programme (FP7/2011-2014) under grant agreement no. 270019
642 (SpaceBook project). The authors would also like to thank Dr Elijah Van Houten for
643 initial discussions on sampling strategies.

644

645 **7 References**

- 646 Andrade, M. V. A., Magalhaes, S. V. G., Magalhaes, M. A., Franklin, W. R. & Cutler, B.
647 M., 2011. Efficient viewshed computation on terrain in external memory.
648 *GeoInformatica*, 15, 381-397.
- 649 Baer, W., Baer, N., Powell, W. & Zografos, J., 2005. Advances in terrain augmented
650 geometric pairing algorithms for operational test. *ITEA Modelling and Simulation*
651 *Workshop*. Las Cruces, NM.
- 652 Bartie, P. & Kumler, M. P., 2010. Route ahead visibility mapping: A method to model
653 how far ahead a motorist may view a designated route. *Journal of Maps*, April
654 2010, 84-95.

- 655 Benedikt, M. L., 1979. To take hold of space: isovists and isovist fields. *Environment and*
656 *Planning B*, 6, 47-65.
- 657 Carver, S. & Washtel, J., 2012. Real-time visibility analysis and rapid viewshed
658 calculation using a voxel-based modelling approach. *GISRUK*. April 6-9,
659 Lancaster University.
- 660 Davidson, D. A., Watson, A. I. & Selman, P. H., 1993. An evaluation of GIS as an aid to
661 the planning of proposed developments in rural areas. In Mather, P. M. (ed.)
662 *Geographical Information Handling: Research and Applications*. London, Wiley.
- 663 De Floriani, L. & Magillo, P., 1994. Visibility algorithms on triangulated digital terrain
664 models. *International Journal of Geographical Information Systems*, 8, 13-41.
- 665 De Floriani, L., Magillo, P. & Puppo, E., 2000. VARIANT: A system for Terrain
666 modeling at variable resolution. *GeoInformatica*, 4, 287-315.
- 667 De Floriani, L., Marzano, P. & Puppo, E., 1994a. Line-of-sight communication on
668 terrain models. *International Journal of Geographical Information Systems*, 8, 329-
669 342.
- 670 De Floriani, L., Montani, C. & Scopigno, R., 1994b. Parallelizing visibility computations
671 on triangulated terrains. *International Journal of Geographical Information Systems*,
672 8, 515-531.
- 673 De Smith, M. J., Goodchild, M. F. & Longley, P., 2007. *Geospatial Analysis: A*
674 *Comprehensive Guide to Principles, Techniques and Software Tools*: Troubador
675 Publishing.
- 676 Fisher-Gewirtzman, D. & Wagner, I. A., 2003. Spatial openness as a practical metric for
677 evaluating built-up environments. *Environment and Planning B: Planning and*
678 *Design*, 30, 37-49.
- 679 Fisher, P. F., 1993. Algorithm and implementation uncertainty in viewshed analysis.
680 *International Journal of Geographical Information Science*, 7, 331-347.
- 681 Fisher, P. F., 1996. Extending the applicability of viewsheds in landscape planning.
682 *Photogrammetric Engineering and Remote Sensing*, 62, 1297-1302.
- 683 Franklin, W. R. & Ray, C. K., 1994. Higher isn't necessarily better: Visibility algorithms
684 and experiments. In Waugh, T. C. & Healey, R. G. (eds.) *Advances in GIS*
685 *Research: Sixth International Symposium on Spatial Data Handling*. London, Taylor
686 and Francis.
- 687 Gal, O. & Doytsher, Y., 2012. Fast and Accurate Visibility Computation in a 3D Urban
688 Environment. *GEOProcessing 2012, The Fourth International Conference on*
689 *Advanced Geographic Information Systems, Applications, and Services*. 105-110.
- 690 Gao, Y., Yu, H., Liu, Y., Liu, Y., Liu, M. & Zhao, Y., 2011. Optimization for viewshed
691 analysis on GPU. *Geoinformatics, 2011 19th International Conference on*. IEEE, 1-5.
- 692 Groves, P. D., 2011. Shadow matching: A new GNSS positioning technique for urban
693 canyons. *Journal of Navigation*, 64, 417-430.

- 694 Kumler, M. P., 1994. An intensive comparison of Triangulated Irregular Networks
695 (TINs) and Digital Elevation Models (DEMs). *Cartographica: The International*
696 *Journal for Geographic Information and Geovisualization*, 31, 1-99.
- 697 Lee, J., 1991. Comparison of existing methods for building triangular irregular
698 network, models of terrain from grid digital elevation models. *International*
699 *Journal of Geographical Information System*, 5, 267-285.
- 700 Lynch, K., 1976. *Managing the sense of a region*: MIT Press Cambridge.
- 701 Mills, K., Fox, G. & Heimbach, R., 1992. Implementing an intervisibility analysis model
702 on a parallel computing system. *Computers & Geosciences*, 18, 1047-1054.
- 703 Rana, S., 2003. Fast approximation of visibility dominance using topographic features
704 as targets and the associated uncertainty. *Photogrammetric Engineering & Remote*
705 *Sensing*, 69, 881-888.
- 706 Rana, S. & Morley, J., 2002. *Optimising visibility analyses using topographic features on the*
707 *terrain*. Available from:
708 <http://www.casa.ucl.ac.uk/publications/workingPaperDetail.asp?ID=44> [23 June
709 2009].
- 710 Salomon, B., Govindaraju, N., Sud, A., Gayle, R., Lin, M., Manocha, D., Butler, B.,
711 Bauer, M., Rodriguez, A. & Eifert, L., 2004. Accelerating line of sight
712 computation using graphics processing units. Place: Published, DTIC
713 Document.
- 714 Seixas, R., Mediano, M. & Gattass, M., 1999. Efficient line-of-sight algorithms for real
715 terrain data. *III SimpÃ³sio de Pesquisa Operacional e IV SimpÃ³sio de LogÃstica da*
716 *Marinha* "SPOLM 1999.
- 717 Stucky, J. L. D., 1998. On applying viewshed analysis for determining least-cost paths
718 on Digital Elevation Models. *International Journal of Geographical Information*
719 *Science*, 12, 891-905.
- 720 Tandy, C. R. V., 1967. The isovist method of landscape survey. In Murray, A. (ed.)
721 *Symposium: Methods of Landscape Analysis*. May 1967, London, England,
722 Landscape Research Group, 9-10.
- 723 Tarel, J.-P., Charbonnier, P., Goulette, F. & Deschaud, J.-E., 2012. 3d road environment
724 modeling applied to visibility mapping: an experimental comparison.
725 *Proceedings of the 2012 IEEE/ACM 16th International Symposium on Distributed*
726 *Simulation and Real Time Applications*. IEEE Computer Society, 19-26.
- 727 Turner, A., Doxa, M., O'Sullivan, D. & Penn, A., 2001. From isovists to visibility graphs:
728 A methodology for the analysis of architectural space. *Environment and Planning*
729 *B: Planning and Design*, 28, 103-121.
- 730 Van Kreveld, M., 1996. Variations on sweep algorithms: efficient computation of
731 extended viewsheds and classifications. In *Proc. 7th Int. Symp. on Spatial Data*
732 *Handling*. Citeseer.

- 733 Wang, J., Robinson, G. J. & White, K., 2000. Generating viewsheds without using
734 sightlines. *Photogrammetric engineering and remote sensing*, 66, 87-90.
- 735 Xia, Y., Li, Y. & Shi, X., 2010. Parallel viewshed analysis on GPU using CUDA.
736 *Computational Science and Optimization (CSO), 2010 Third International Joint*
737 *Conference on*. IEEE, 373-374.
- 738 Ying, S., Li, L., Mei, Y. & Peng, X., 2006. Incremental terrain visibility analysis.
739 *Proceedings of SPIE - The International Society for Optical Engineering*. 28 October
740 2006, Wuhan, SPIE.
- 741
- 742